UKAEA FUS 362

UKAEA

Fusion
(UKAEA/Euratom Fusion Association)

Neoclassical Islands on COMPASS-D

D A Gates et al

To be Submitted to Nuclear Fusion

March 1997

UKAEA
Fusion

Culham, Abingdon
Oxfordshire OX14 3DB
United Kingdom
Telephone 01235 464131
Facsimile 01235 463647

Neoclassical Islands on COMPASS-D

D. A. Gates, B. Lloyd, A. W. Morris, G. McArdle, M. O'Brien, M. Valovic,
C. D. Warrick, H. R. Wilson and the COMPASS-D and ECRH Teams
UKAEA, Fusion, Culham, Abingdon, Oxon, OX14 3DB, UK.
(UKAEA/EURATOM Fusion Association)

Abstract

Neoclassical magnetic islands are observed to limit the achievable β in COMPASS-D low collisionality single-null divertor tokamak plasmas with ITER-like geometry (R_0=0.56m, B_0 =1.2T, I_p=120-180kA, κ=1.6, ε=0.3). The limiting β is typically well below that expected from ideal instabilities with maximum β_N in the range of 1.6-2.1. The plasma is heated with up to 1.8MW of 60GHz ECRH at 2nd harmonic with X-mode polarisation. The time history of the measured island width is compared to the predictions of neoclassical tearing mode theory, with good agreement between theory and experiment. The measured islands have a threshold island width below which the mode will not grow. The density scaling of the point of onset of the measured instabilities is compared to two theories which predict a threshold island width for the onset of neoclassical tearing modes. Applied resonant helical error fields are used to induce islands in collisionality regimes wherein the neoclassical islands do not occur naturally, allowing the study of the behaviour of neoclassical tearing modes in this regime. The critical β for the onset of neoclassical tearing modes is seen to be ~3 times higher in the naturally stable region. This observation is compared to the predictions of both threshold theories. A simple expression for the q-scaling of the maximum achievable β_N in the presence of neoclassical tearing modes is derived based on the assumption of a maximum allowable island width. The predicted q-scaling of this β-limit is compared to data from a q-scan and the results are in good agreement.

1. Introduction

Much attention has been focused recently upon tokamak operational pressure limits imposed by non-ideal MHD instabilities, in particular the effects of bootstrap current driven magnetic islands. This is primarily due to the observation on several divertor tokamaks that the β limit at low density (and hence low collisionality) is often determined either by locked or rotating magnetic islands, typically at a value of β below the Troyon limit [1] imposed by ideal instabilities. This effect has been observed on COMPASS-D [2], DIII-D [3], and ASDEX-U [4]. Neoclassical tearing modes have also been identified as a possible β-limiting phenomenon on JT-60U [5]. Initial calculations of the stability of bootstrap driven islands [6,7] indicated that these modes were unstable for all values of β_p when the collisionality was sufficiently low for the bootstrap current to flow. More recent calculations, motivated by the observation of a critical island width on TFTR [8] (where neoclassical tearing modes were first positively identified), suggest that other stabilising mechanisms are important in determining the onset of these modes.

In section 2 we present a brief review of the theory of neoclassical tearing modes. We also describe the general behaviour of the equation governing the growth of these modes in section 3, making distinctions between the various terms.

In section 4, we discuss the applicability of the neoclassical tearing mode island evolution equation to the observed instabilities on COMPASS-D. In particular, it will be shown that the time evolution of the width of an m=2 magnetic island (as calculated from the measured perturbed radial n = odd magnetic field) during a power ramp down experiment is well described by the theoretical model using experimental inputs to determine the important free parameters. Also, we discuss the behaviour of the mode at small amplitude and confirm the existence of an island threshold, as in Ref. [8].

Threshold mechanisms are discussed in sections 5, 6, 7, and 8. To date, there are two proposed stabilisation mechanisms which could explain the observed threshold: one based on a model of the transport through the island [9], called the $\chi_\perp/\chi_{||}$ model, the other on the effect of ion polarisation currents [10,11]. The implications of these models will be discussed and the predictions compared to a series of high β discharges on COMPASS-D for which the density was varied while all other externally controllable parameters were held fixed.

Section 9 covers an experiment which measures the critical β for instability. COMPASS-D is well equipped with a set of readily configured quasi-helical windings, allowing the generation of artificial error fields. Applied resonant helical error fields are used to induce islands in higher collisionality regimes wherein the neoclassical islands do not occur naturally (i.e. the threshold for instability is not exceeded by the plasma perturbations present or the modes are inherently stable), allowing the study of the behaviour of neoclassical tearing modes in this regime. Experiments with applied resonant helical error fields indicate that the threshold error field for penetration is a function of β in the regime where these modes are naturally stable. Additionally, the results of a power scan at (relatively) high density shows that there is a critical β for the onset of these modes even when the modes are not excited naturally.

Lastly, in section 10, we investigate the effects of bootstrap driven islands on the operational β limit assuming that it is these modes that determine the maximum achievable β in low collisionality tokamaks. A simple scaling law for the q dependence of the β-limit is derived based on the assumption that the maximum allowable island width is determined by the distance from the rational surface either to the q=1 surface or to the plasma boundary. A β limit is immediately attained from this assumption since the saturated neoclassical island width is proportional to β_p. A distinction is made between the case wherein the instability threshold is crossed while the β is low and the case where the β is already above the β-limit imposed by saturated neoclassical islands.

2. Theory

It is important to understand the physics underlying the occurrence of the low m/n islands that are observed to limit β so that the regime where these modes are dominant can be avoided in the future, if possible. A strong candidate for the driving mechanism behind these islands is the bootstrap current. The mechanism is simple to understand; at high β_p and low ν_* the pressure gradient in the plasma gives rise to the bootstrap current. If an island, develops the pressure within the island tends to flatten, thereby removing the drive for the bootstrap current. This gives rise to a helical "hole" in the bootstrap current, which increases the size of the island. The equation for the

island width, including the bootstrap current drive term and the usual current gradient drive (from Rutherford theory), is given by:

$$\frac{dw}{dt} = \left(\frac{1.22\eta_{nc}}{\mu_0}\right)\left[\Delta' + a_1\varepsilon^{1/2}\left(\frac{L_q}{L_p}\right)\frac{\beta_p}{w}\right] \qquad (1)$$

where w = island width, η_{nc} is the neoclassical resistivity, Δ' is the jump in the logarithmic derivative of the perturbed flux (representing the current gradient drive), a_1 is a constant that depends on the details of the equilibrium, $\varepsilon \equiv r_s/R$, is the inverse aspect ratio of the rational surface, $\beta_p = 2\mu_0 p(r_s)/\langle B_\theta\rangle^2$, is the local poloidal β ($p(r_s)$ is the pressure, $\langle B_\theta\rangle$ is the poloidal magnetic field averaged around the plasma poloidal circumference), $L_q = q/q'$, is the local gradient scale length of the safety factor q, and $L_p = p/p'$, is the local gradient scale length of the pressure (all quantities to be evaluated at the rational surface of interest, $r=r_s$, where $m = nq(r_s)$).

It is clear that Equation (1) predicts that an island will always be present, since for sufficiently small w, the second term will dominate the first, even if the first is strongly negative. For negative Δ' this equation predicts a saturated island width, w_{sat}, given by:

$$w_{sat} = -a_1\varepsilon^{1/2}\left(\frac{L_q}{L_p}\right)\frac{\beta_p}{\Delta'} \qquad (2)$$

Clearly, since tokamak plasmas do not always have magnetic islands, there must be some mechanism that mitigates the effect of the bootstrap drive term. To date two stabilising mechanisms have been proposed which stabilise this mode at small island width. With these terms included, Equation (1) becomes:

$$\frac{dw}{dt} = \left(\frac{1.22\eta_{nc}}{\mu_0}\right)\left[\Delta' + a_1\varepsilon^{1/2}\beta_p\frac{L_q}{L_p}\left(\frac{w}{w^2+w_c^2}\right) - a_2\frac{\rho_{\theta i}^2\beta_p g(\varepsilon)}{w^3}\left(\frac{L_q}{L_p}\right)^2\right] \equiv f(w) \qquad (3)$$

(all quantities to be evaluated at the rational surface) Here a_2 is a coefficient which depends on the details of the equilibrium. The second term on the right is the bootstrap island term modified to include the effects of transport across the island, with w_c [9] parameterising the magnitude of the contribution of the $\chi_\perp/\chi_{||}$ model and given by the relation:

$$w_c = 1.8r_s\sqrt{\frac{8R_0L_q}{r_s^2 n}\left(\frac{\chi_\perp}{\chi_{||}}\right)^{1/4}} \qquad (4)$$

The third term [10,11] in Equation (3) is the contribution due to ion polarisation currents, with $\rho_{\theta i}$ = the poloidal ion Larmor radius, and $g(\varepsilon)$ defined by:

$$g(\varepsilon) = \begin{cases} \varepsilon^{3/2} & for\ \ \nu_i/\varepsilon\omega_{*e} << 1 \\ 1 & for\ \ \nu_i/\varepsilon\omega_{*e} >> 1 \end{cases} \qquad (5)$$

where $\nu_i = 2.72\text{x}10^{-17} n_e Z^4 T_i^{-3/2}$ is the ion collision frequency (Z is the effective ion charge, T_i is measured in keV, and n_e in unit of m^{-3}), and $\omega_{*e} = 9.97\text{x}10^3 mT_e/(r_s L_p B_\phi)$ is the electron diamagnetic frequency.

The physical origin of the $\chi_\perp/\chi_{||}$ term can be understood as a reduction in the bootstrap current due to incomplete flattening of the pressure profile. The flattening of the pressure within an island is due to the flux of energy along field lines within an island, which connect the inner and outer sides of the island interior (i.e. $r< r_s$ and $r>r_s$, respectively). If this parallel flux fails to dominate the flux of energy across field lines, the pressure will not completely flatten. Since it is the pressure gradient that drives the bootstrap current and it is the "hole" in the bootstrap current that drives the island, the reduced flattening reduces the drive for the instability.

The ion polarisation current arises due to the rotation of the island within the plasma relative to the frame where the mean radial electric field vanishes. This gives rise to an inductive electric field. Along island flux surfaces, this electric field is short circuited by the electron response (that is an electrostatic potential is formed which cancels the parallel component of the induced electric field). This potential in turn creates a radial electric field, as a result of the island geometry.

In the collisional regime (the word collisional here means that the effective ion collision frequency, ν_i/ε, is large relative to the island rotation frequency as measured in the plasma frame, ω, i.e. $\nu_i/\varepsilon\omega >>1$, where it will be assumed that $\omega \sim \omega_{*_e}$), the radial component of the electric field gives rise to a purely toroidal ion flow, since the poloidal flow is strongly damped by collisions. Since the radial electric field is varying in time, the toroidal ExB drift velocity induced by the island also varies in time. It is this time varying toroidal ExB drift that gives rise to the radial polarisation current. Quasi-neutrality then implies a parallel current which either helps stabilise or destabilise the island, depending on the direction of mode rotation relative to the plasma frame.

In the collisionless regime the argument is similar, but instead of all the particles "seeing" the time varying radial electric field, only the trapped particles are affected. This is because the mode now makes a complete toroidal transit of the plasma (in the plasma frame) before the average ion has a collision, thus averaging the effect of the mode on passing particles. Therefore, the radial polarisation current for these particles will average to zero on an island flux surface. The contribution of the polarisation current in the collisionless regime is reduced by a factor of $\varepsilon^{3/2}$ as in Equation (5).

3. General Behaviour

A plot of the typical behaviour of $f(w)$ from Equation (3) is shown in Figure 1. Also shown is the curve predicted by Equation (1). The addition of the new terms has created a region of stability (i.e. $dw/dt < 0$) at small island widths. If the additional terms in Equation (3) accurately represent the physics which determines mode stability at small island width, then small magnetic islands are never truly unstable. Instead, the axisymmetric equilibrium is a metastable state. If a perturbation exists that is large enough to create an island at least as large as the critical island width defined by the left most intersection of the curve with the $dw/dt = 0$ axis in Figure 1, then the island will grow to a saturated value determined by the rightmost intersection of the curve with the $dw/dt =0$ axis. Note that the saturated island width is very close to that predicted by Equation (1), in accordance with the observations in Reference [8]. This is because the effects of both stabilising terms are only important for small island widths, and hence they do not significantly affect the large island steady-state solution.

It is useful to study the effects of each of the two additional terms in Equation (3) separately. Typical $f(w)$ curves for the case $w_c = 0$ are shown in Figure 2a, while the curves for $a_2=0$ are shown in Figure 2b. Shown in Figure 2c is the effect of crossing the collisionality boundary for the function $g(\varepsilon)$ for the case with $w_c = 0$ and $a_2 > 0$. At low collisionality the threshold island width is a factor $\varepsilon^{3/4}$ smaller than it is at high collisionality. There are a few key features to note: a) the critical island width for the curves in Figure 2b rapidly approaches zero for increasing β_p (assuming fixed w_c, which is fairly realistic given the weak parametric dependence of w_c), b) the critical island width in Figure 2a is primarily a function of the ion poloidal gyro-radius, $\rho_{\theta i}$ c) the curves in Figure 2c have a more complicated behaviour with collisionality as a result of the function $g(\varepsilon)$.

4. Experiment 1 - Quasi Steady State Island Dynamics

The simplest aspect of Equation (3) to verify for the low *m/n* islands observed to limit β_p on COMPASS-D is that the time history of the measured island width has the same scaling with plasma pressure as that predicted for the quasi-steady state solution. As already stated, uncertainty in the threshold mechanism that is responsible for the onset of MHD is unimportant if the island has already saturated. Therefore, the approach adopted is to create a large saturated island and then reduce the input power, whereupon we observe the response of the island to the subsequent reduction in β_p.

The target plasmas were single null divertor discharges with ITER-like geometry (R_0=0.56m, B_0 =1.2T, I_p = 150kA, κ=1.6, ε=0.3). The q_{95} for these discharges is 4.3, since it was not possible to operate reliably at ITER-like values of q_{95} ($q_{95} \sim 3$) due the increased disruption frequency induced by the appearance of these modes. The plasmas are heated with up to 1.8MW of 60GHz ECRH at second harmonic with X-mode polarisation. Figure 3 shows an equilibrium reconstruction of an example discharge. Also shown in the Figure are the ECRH rays as traced by the BANDIT3D Fokker-Planck code [12] showing the absorption pattern expected for the different ECRH antennae. Figure 4a shows the measured perturbed field amplitude for such a discharge. Figure 4b shows the time history of input power and β_p (as measured by diamagnetic loop). Figure 4c shows the resulting island width which was obtained using the approximate cylindrical formula:

$$w = 4r_s\sqrt{\frac{q}{m\varepsilon}\left(\frac{L_q}{r_s}\right)\left(\frac{b}{r_s}\right)^{m+1}\sqrt{1+(\omega\tau_w)^2}\,\frac{\tilde{B}_r(b)}{B_\phi}} \qquad (6)$$

where b is the effective radius of the vacuum vessel, $\tilde{B}_r(b)$ is the perturbed radial magnetic field measured at the wall, and, $\tau_w \equiv (1 - (r_s/b)^{2m})\mu_0\sigma r_w\delta/2m$, is the effective resistive wall time which is ~ $210\mu s$ for COMPASS-D. The result is the overlaid with the island width calculated from a code which solves Equation (3). The coefficients used in the calculation are $r_s\Delta' = -2.0$, $a_1 = a_2 = 7.0$. Note that similar results can be obtained for various combinations of the values of w_c and a_2 since these parameters are not well determined by the power ramp-down experiment. The key points are that a) the island width is roughly linearly dependent on β_p as predicted by Equation (2), and b) there is a delay in the decay in island width relative to the decay in β_p that is

consistent with that predicted by resistive diffusion. The data is therefore consistent with the mode being a neoclassical island.

5. Experiment 2 - Transient Island Dynamics

We can now consider in detail what happens in the experiment at the point of onset of MHD and try to compare these predictions. Figure 5 shows the time evolution of an example discharge in a density scan, for which the density was varied between $4.4\text{x}10^{18}\text{m}^{-3}$ and $1.2\text{x}10^{19}\text{m}^{-3}$. The typical equilibrium parameters for the discharges in the scan are I_p = 150kA, B_ϕ = 1.2T, a = 0.17m, R_0 = 0.56m, q_{95} = 4.3, κ = 1.6 with ITER-like single null divertor geometry, as in the previous section. The ECRH power was turned on and ramped to its maximum value (0.8 - 1.2MW). The individual gyrotrons were turned on at intervals exceeding 20ms starting at t ~100ms.

Figure 6 shows the Mirnov activity as measured by the outboard midplane Mirnov coil for several of the shots in the scan. As the density is raised the onset of the MHD is delayed progressively until it ceases to appear. Since the time history of β_p is very similar and ramping for all the discharges, this means the value of β_p at which the mode appears increases. The line average density and β_p at the point of MHD onset is shown inset in each plot.

The data from the density scan is analysed near the point of onset of MHD. Figure 7a shows the typical early time history of the observed 2/1 mode for a single Mirnov coil, while Figure 7b shows the RMS component of the perturbed poloidal field from 12 Mirnov coils summed in such a way as to optimally enhance the signal to noise ratio for a 2/1 mode. This shows qualitatively the behaviour expected from Equation (3). In particular, the signal suddenly appears from the noise, excited by a sawtooth to finite amplitude. The mode then hovers around the "critical" island width for a period and then the growth of the mode rapidly increases (as predicted by the curves in Figure 2). The island then grows until it saturates at an amplitude that is determined by Equation (2) (i.e. proportional to β_p). Alternatively, the data from Figure 7 can be displayed on the axes in Figure 1 by taking the derivative of the square root of the poloidal field (which is proportional to the island width) and plotting vs. the island width. Figure 8 shows such a plot. One can see that the curve traced out by the island as it grows is qualitatively similar to that predicted by Figure 2. The numbered points in Figure 8 correspond to the similarly marked points in Figure 7, to give an idea of the temporal correspondence between the different curves. The normalisation of the predicted curve is chosen so as to best fit the data, but the maximum growth rate is roughly consistent with that calculated using neoclassical resistivity.

6. Thresholds

Since there is both a critical β_p, β_{pcrit}, and a critical island width, w_{crit}, for the onset of MHD, as well as a "seed" perturbation, w_{seed}, required to drive the island initially, one can reasonably ask which quantity(ies) is (are) varying so as to give rise to the strong variation in the onset of MHD apparent in Figure 6. The growth rate of the island as a function of β_p is an important indicator as to the mechanism behind the onset

of MHD. If one accepts that Equation (3) describes the island evolution, then it is possible to show that the boundary that is being crossed is the $w_{seed} > w_{crit}$ boundary, rather than the $\beta_p > \beta_{pcrit}$ boundary.

One thing that is clear regardless of threshold mechanism, is that if the threshold that is being crossed is the threshold in β_p then the mode would appear with a very small growth rate. This is evident from Figure 2 which shows that the value of *dw/dt* is zero at the critical β_p (by definition). The data in Figure 6 shows the measured Mirnov amplitude for the sequence of discharges from the density scan. For the shot at the lowest density, the initial growth is small, and the island size grows roughly proportional to β_p, consistent with an instability onset near the critical β_p. However, as the density is raised the initial mode growth is increasingly strong, indicating that β_p is already significantly above the critical value. Therefore the threshold that is being crossed must be the $w_{seed} > w_{crit}$ threshold.

Assuming that the relevant threshold is indeed the threshold in island width rather than the threshold in β_p, the question still remains as to whether the observed strong variation in the onset of MHD is caused by the variation in w_{crit} or, instead, by the variation in w_{seed}. This can be addressed by studying the behaviour of the mode at small amplitude as a function of density. The values of the measured threshold island width (determined using plots similar to Figure 6) for the series of shots in the density scan presented in Section 5 are plotted against density and β_p in Figure 9. There is no clear scaling of the measured threshold with density or β_p. This indicates that the variations in the magnitude of the transient events which trigger instability, i.e. the source of w_{seed}, which on COMPASS-D is primarily sawteeth (these discharges do not have Edge Localised Modes [ELMs] and do not show any of the usual signs of H-Mode, but the confinement is high, see Reference [2]), are not responsible for the strong scaling in the onset of MHD with density. The only remaining possibility (within the context of this analysis) is that w_{crit} varies strongly with density. The picture is then that a roughly constant "bath" of perturbations exists due to other perturbations such as frequent sawteeth and w_{crit} is varying during the discharge. When w_{crit} becomes smaller than the available perturbation, which is roughly constant, the neoclassical island will grow.

7. Threshold Scalings

In order to compare the measured results with the predictions of the theories described in the introduction it is first necessary to determine the size of the island threshold and what density scalings are to be expected for the onset of MHD according to the differing paradigms.

First we point out that both models predict that there is a critical β_p below which the mode is always stable. For the ion polarisation current model the critical β_p can be expressed as:

$$\beta_{pcrit} = -\frac{3\sqrt{3}}{2}\left(\frac{L_p}{L_q}\right)^{1/2} f(\varepsilon)\Delta' \rho_{\theta i} \qquad (7)$$

where we have taken $a_2/a_1 = 1$ (in accordance with Section 4) and with:

$$f(\varepsilon)=\begin{cases} 1 & \nu_i/\varepsilon\omega_{*_e} << 1 \\ \varepsilon^{-3/4} & \nu_i/\varepsilon\omega_{*_e} >> 1 \end{cases} \tag{8}$$

For the $\chi_\perp/\chi_{||}$ model the expression is:

$$\beta_{pcrit} = -\frac{3\sqrt{2}}{2a_1} f(\varepsilon)\left(\frac{L_p}{L_q}\right)\Delta' w_c \tag{9}$$

As already stated, both models also predict critical island widths which must be exceeded for the mode to grow. Assuming $\beta_p >> \beta_{pcrit}$, the critical island width for the ion polarisation threshold of Reference [17] gives:

$$w_{crit} = \sqrt{\varepsilon} f(\varepsilon)\left(\frac{L_q}{L_p}\right)^{1/2} \rho_{\theta i} \tag{10}$$

When this quantity becomes less than the available seed island width, which is roughly constant, the mode will grow. For COMPASS-D high β discharges, which are heated with high power ECRH, Neutral Particle Analyser (NPA) measurements of the ion temperature indicate that T_i remains roughly constant as the heating power is increased in time, implying that $\rho_{\theta i}$ also remains roughly constant. This, combined with the assumption that L_p/L_q does not change significantly during the current flattop portion of the discharge, implies that the only significant variation of w_{crit} is due to the change in the "collisionality-like" parameter $\nu_i/\varepsilon\omega_{*pe}$. Therefore, the onset of MHD is possible only if this parameter falls below ~ 1 during the discharge, and $\beta_p > \beta_{pcrit}$. This parameter can be written:

$$\frac{\nu_i}{\varepsilon\omega_{*pe}} = 2.73\frac{r_s L_n n_{20} B}{\varepsilon m T_e T_i^{3/2} \mu^{1/2}} \propto \frac{n}{T_e} \tag{11}$$

with μ = ion mass in AMU's.

We will make the further assumption that T_e at the rational surface scales with the globally measured diamagnetic β_p, $\beta_p(a)$, (i.e. the density and temperature profiles do not vary greatly during a discharge). Equation (11) then becomes, for $\beta_p > \beta_{pcrit}$:

$$\frac{n^2}{\beta_p(a)} = const. \qquad or \qquad \beta_p(a) \propto n^2 \tag{12}$$

For the $\chi_\perp/\chi_{||}$ model of Reference [9], it is more difficult to determine the scaling of the onset of MHD activity with plasma parameters such as density due to the uncertainty in choosing a perpendicular diffusivity that is appropriate for transport across an island. Therefore we adopt a different approach: determine the size of the critical island threshold and infer from the data how the diffusivity must scale with density. This scaling can then be compared with known confinement time scaling laws.

The collisionless expression for parallel diffusivity used in Reference [9] (see paragraph following Equation (2) of the reference) is the most appropriate for

COMPASS-D data. The condition that determines whether one should use the collisional form of $\chi_{||}$ as opposed to the collisionless form can be expressed as:

$$\lambda_{mfp} < \lambda_{||} \tag{13}$$

where λ_{mfp} is the mean free path for collisions and $\lambda_{||} \equiv R_0 q L_q/(mw)$ is the effective parallel wavelength of the mode. This condition can similarly be expressed as:

$$\chi_{||(collisional)} \equiv v_{the}\lambda_{mfp} < v_{the}\lambda_{||} \equiv \chi_{||collisionless} \tag{14}$$

where $v_{the} \equiv \sqrt{2kT_e/m_e}$ is the electron thermal velocity. The parameters for 2nd harmonic ECRH heated discharges on COMPASS-D are such that the collisionless form for $\chi_{||}$ is always smaller than the collisional form. Hence the collisionless $\chi_{||}$ is the appropriate form to adopt.

Using this result, one can show that the critical island width for instability at $\beta_p = \beta_{pcrit}$ can be written:

$$w_{crit}(\beta_{pcrit}) = 5.5 r_s \left(\frac{\chi_\perp}{r_s v_{the}} \frac{L_q}{n\varepsilon^2 R_0} \right)^{1/3} \tag{15}$$

where m is the poloidal mode number. This expression, albeit using the collisional form of the parallel diffusivity, has been used to estimate the value of the critical island width on other experiments (see References [3] and [13]). However, as we have demonstrated, $\beta_p >> \beta_{pcrit}$ at the point of onset of MHD in almost all cases observed in experiment. The correct expression for the critical island width when β_p is well above the critical value is:

$$w_{crit} = \frac{207.4 r_s}{a_1^2} \left(\frac{\Delta' r_s}{\varepsilon \beta_p} \right)^2 \left(\frac{\chi_\perp}{r_s v_{the}} \right) \left(\frac{L_p^2}{r_s L_q} \right) \tag{16}$$

as in Equation 126 from Reference [9].

If one now makes the same assertion as above, namely that the source of seed island is approximately constant for all plasmas (i.e. that the onset of MHD corresponds to a fixed value of w_{crit}, i.e. when w_{crit} = const.), then one finds at the onset of MHD activity:

$$\beta_p \propto n^{1/5} \chi_\perp^{2/5} \tag{17}$$

Since there is no clear reason to choose any particular scaling of the perpendicular energy transport with β_p and density we instead attempt to determine the scaling required to fit the data. We assume that the energy diffusivity scales as some power of density and β_p, that is $\chi_\perp \propto n^\alpha \beta_p^\gamma$. In order to match a scaling of $\beta_p \, \alpha \, n^d$ (similar to the scaling in Equation (12)) at the point of onset of MHD one finds:

$$\chi_\perp \propto n^\alpha \beta_p^{[(5d-1)/2d]-\alpha/d} \tag{18}$$

with α a free parameter and d determined by experiment.

8. Comparison of Threshold scalings to Experiment

The regions in Figure 10 represent the various boundaries which arise as the result of the ion polarisation current scalings for the onset of MHD. The horizontal lines in Figure 10 represent the values of β_{pcrit} as determined by Equation (7). The upper line represents the critical β_p at high collisionality and the lower line is for low collisionality. The parabolic curve is the transition from low to high collisionality determined by Equation (11). Overlaid on this figure are the values of density and $\beta_p(a)$ at the point of onset of MHD from the density scan described in Section 5. The ratio of $\beta_p(a)$ to β_p is calculated assuming parabolic density temperature and q-profiles.

The size of the threshold for the polarisation current model as calculated from the collisionless form of Equation (10), using the values; $L_p/L_q \sim 1$, $T_i = 0.15$keV, $B_\phi = 1.2$T, q=2, $r_s = 0.13$m, $R_0 = 0.56$m, $\mu = 2$ and the definition:

$$\rho_{\theta i} = 4.57x10^{-3}\frac{q\sqrt{\mu T_i}}{\varepsilon B_\phi} \quad (m) \tag{19}$$

gives $w_{crit} = 1.0$cm in reasonable agreement with the observed threshold of ~1.5cm as seen in Figure 9.

Turning to the $\chi_\perp/\chi_{||}$ model, it is very difficult to choose α with the constraints given in Equation (18) such that the perpendicular energy diffusivity scales as that measured from the global energy confinement time on COMPASS-D with $1 < d < 3$ particularly since in these hot electron plasmas the energy confinement is not observed to vary with either β_p or density. In particular, if one chooses $d = 2$, as for the ion polarisation current model, one finds that in order to match global scaling laws ($\chi_\perp \sim \beta$) that α=2.5, a very strong function of the density. Alternatively, if one chooses α small (~1/3) in accordance with the observed independence of τ_E on density then d must also be small (~0.55) in contradiction with the data in Figure 10. However it is not possible to rule out this scaling law based on such arguments since one cannot necessarily assume that the confinement within an island will scale similarly to that in the bulk plasma.

However, one can calculate the absolute value seed island width required for instability for typical COMPASS-D parameters and one finds that the size of the predicted seed island is quite small, in particular:

$$w_{crit} < 2.9x10^{-5}\frac{\chi_\perp}{\beta_p^2\sqrt{T_e(keV)}} < 0.5mm \tag{20}$$

again assuming $\chi_\perp \sim 1\text{m}^2/\text{s}$. This is substantially below that observed in experiment. It should also be pointed out that we have chosen a very favourable model for $\chi_{||}$ and, due to the insensitivity of the model to changes in the assumed transport coefficients, it is quite difficult to imagine that small changes to the parameters used could bridge the gap between the measured and predicted values.

9. Experiment 3 - Critical β

An important issue for understanding the onset of bootstrap driven island is the determination of the relative magnitude of the two "threshold" terms in Equation (3). One important difference between the terms is the collisionality scaling of the w_{crit} threshold, which is discussed at length in Sections 7 and 8. However, a stronger distinction can be made if one considers the collisionality dependence of the critical β_p. Both equations give roughly similar numerical values of $\beta_{pcrit} \sim 0.2$ (assuming the collisionless case for the ion polarisation current model, and that $\chi_\perp \sim 1\text{m}^2/\text{s}$ and $\chi_{||} = v_{the}\lambda_{||} = v_{the}R_0qL_q/(mw)$ for the $\chi_\perp/\chi_{||}$ model). Comparing Equations (7) and (9), the function $g(\varepsilon)$ in the ion polarisation current implies that there should be a rapid change in the magnitude of the β_{pcrit} for a small change in collisionality (i.e. density). On the other hand, the dependence on collisionality for the $\chi_\perp/\chi_{||}$ model is expected to be relatively weak.

However, as already stated, the intrinsic plasma perturbations are not sufficient to drive instability when $\beta_p = \beta_{pcrit}$ and $\nu_i/\varepsilon\omega_{*_e} > 0.3$. Fortunately, using the extensive set of error field windings available on COMPASS-D [14] , it is possible to induce an island. If the error field is then turned off, the island should either persist or decay depending on whether β_p is above or below the critical value. The applied error field acts as a probe to test the depth of the well for the metastable axisymmetric equilibrium.

A series of experiments were undertaken to test this measurable difference between the two threshold models. In discharges similar to those previously described, (i.e. I_p = 150kA, B_ϕ = 1.2T, a = 0.17m, R_0 = 0.56m, q_{95} = 4.3, κ = 1.6 with ITER-like single null divertor geometry) the ECRH power is rapidly ramped to full value and, simultaneously a large error field is applied. (The error field configuration applied has predominantly m=2, n=1 structure giving 3.5 Gauss of resonant radial field at the rational surface in vacuo. Typically, 2.5kA of current flow through the coils in this experiment giving ~10.5Gauss of 2/1 radial field at the rational surface.) The error field is then turned off. The behaviour of the measured field from the induced island as a function of time for varying β_p is shown in Figure 11a-d. At low β_p (Figure 11a) it is not possible to induce a mode. The mode structure is predominantly m=2/n=1. For intermediate β_p the mode appears but decays. At the highest β_p (Figure 11d) the mode persists. The behaviour is wholly consistent with $\beta_{pcrit} \sim 0.6$. However, as demonstrated in Figure 10, naturally occurring modes (represented by solid circles) are present for $\beta_p \sim 0.2$ when the density is reduced by only a factor of 2. This is a very strong dependence of the critical β_p on plasma density that cannot be explained by the weak collisionality scaling of the $\chi_\perp/\chi_{||}$ model, i.e. of w_c (See Equation (4) above).

An additional interesting result, which is not yet well described by theory, is obtained by measuring the current required to induce a locked mode as a function of β_p and density within the region that is not naturally subject to neoclassical islands on COMPASS-D, that is the high collisionality region to the right of the parabolic curve in Figure 10. This result, also reported in Reference [15], is a possible explanation for the "error field mode" on JET reported in Reference [16]. Shown in Figure 12 is the density and β_p at which the onset of non-rotating MHD was observed from a series of discharges for which β_p was quickly ramped to a constant value and the error field (using the coil configuration described above) slowly ramped until a locked mode

appeared. The solid triangles represent modes that were induced with error field currents less than 1.5kA and solid squares represent modes that required greater than 1.5kA of error field current to be induced. The striped area in the figure represents the region where $\beta_p > \beta_{pcrit} = 0.6$ in the collisional regime (i.e. $\nu_i/\varepsilon\omega_{*e} > 0.3$, where we have chosen 0.3 as the point at which the collisionality becomes low for consistency with Reference [17]). There is an inverse correlation between the amount of required current to induce a mode and β_p. The data from Figure 10 (solid circles) is also shown in Figure 12 for reference.

10. q-scaling of the β-limit

If the neoclassical islands are present in a tokamak discharge, they will eventually limit the achievable plasma pressure. This is evident from Equation (2). The saturated island size is proportional to β_p. Therefore, there is a maximum achievable pressure determined by the maximum allowable island size. There are two scenarios possible for reaching this limit. The first is that the threshold for instability is not crossed until β_p is already greater than the maximum β_p allowed in the presence of neoclassical islands. In this case the island would grow rapidly and β_p would either drop or the plasma would disrupt. β_p can therefore exceed the limit imposed by neoclassical islands until the modes can be excited. The second scenario is where the mode is excited at a value of β_p below the maximum β_p allowed in the presence of an island. In this case the mode would rapidly grow to the saturated size. If the pressure was then increased further, the mode would grow slowly up to the maximum allowed width, with the island width proportional to β_p.

Considering the second case described above, one can calculate the limit to β imposed by neoclassical tearing modes. The simple model proposed here is that the β limit is determined by the saturated bootstrap driven island interacting either with the q=1 surface or with the plasma edge. This can be simply stated as:

$$w_{max} = \alpha Min[r_s - r_{q=1}, a - r_s] \tag{21}$$

which gives:

$$\beta_{pmax} = -\frac{\Delta' L_p}{\varepsilon^{1/2} L_q} Min[\alpha(r_s - r_{q=1}), \gamma(a - r_s)] \tag{22}$$

where α and γ are the fractional island widths required for interaction with the q=1 surface and the plasma edge, respectively.

A simple scaling of the β-limit with q is obtainable by assuming a specific form for the q-profile. For simplicity we assume a quadratic form, $q = q_0 + (r/a)^2(q_a - q_0)$. Solving for r_s and substituting the definition of $\beta_N (\equiv 20\beta_p(a)/Aq_a$, $A \equiv R/a)$:

$$\beta_{Nmax} = \frac{20(-\alpha r_s \Delta')}{A^{1/2}} \left[\frac{\langle p \rangle L_p}{p_{r_s} L_q}\right] \frac{q_a}{q^2} \left(\frac{q - q_0}{q_a - q_0}\right)^{3/4} Min\left[1 - \sqrt{\frac{1 - q_0}{q - q_0}}, \delta\left(\sqrt{\frac{q_a - q_0}{q - q_0}} - 1\right)\right] \tag{23}$$

where $\delta = \gamma/\alpha$, $<p>$ is the volume averaged pressure, and p_{r_s} is the pressure at the rational surface.

Figure 13 shows the overlay of the curves predicted by Equation (23) as calculated with data from COMPASS-D. The relevant mode is assumed to be m/n=2/1 for COMPASS-D, consistent with observation. The terms which do not have explicit q dependence in Equation (23) are assumed to be roughly independent of q, and q_0 = 0.95 and $\delta = 1$, are also assumed. $\alpha r_s \Delta'$ is assumed unknown and is used as a fitting parameter to the envelope of the data.

One can easily imagine more complicated models based on the same physics. For example one might wish to include the effect of multiple islands or the q-scaling of the plasma scale lengths or more realistic q-profiles. However, the simple model presented here is sufficient to describe the scaling of the COMPASS-D experimental data with reasonable accuracy.

It should also be stressed that the pressure limit indicated in Equation (23) is only applicable if the neoclassical mode is excited. It does not represent the absolute limit to β. Higher normalised β's have been achieved in COMPASS-D with various methods (see for example Reference [2]). If, however, this limit is exceeded and then a mode is excited, β must either drop to a value below this limit or the plasma will disrupt.

11. Summary

The dynamics of the low m/n magnetic islands that limit the operationally achievable β in COMPASS-D have been investigated and are found to be broadly consistent with the predictions of neoclassical tearing mode theory. The quasi-steady state island width is found to be proportional to β_p as predicted by the bootstrap current drive for the mode. The transient evolution is found to be consistent with crossing a critical island threshold, rather than a threshold in β_p. Also, the transient island growth shows good qualitative agreement with that predicted by the neoclassical island evolution equation.

The islands are observed to exhibit threshold behaviour, requiring a seed perturbation in order to grow, as originally observed in Reference [8]. The scaling of the size of the island width threshold has been shown to be the cause of the scaling of the onset of MHD activity. The hypothesis that it is the scaling of the critical β_p that determines the onset of the modes is inconsistent with observations. The scaling of the size of the available seed perturbation also cannot explain the measured scaling of the onset of MHD.

Two theories which predict a critical island threshold width for instability of the neoclassical bootstrap current driven island have been examined and compared to data from a COMPASS-D density scan performed at high β. The first model, based on the effects of ion polarisation currents, shows both the correct size for the threshold and the appropriate scaling with β and density to explain the observed results. The second model, based on the assumption that the important effect is the lack of equilibration of electron temperature along perturbed flux surfaces, is indeterminate in terms of the

scaling of the onset of MHD with density and temperature since the scaling of the perpendicular transport across the island with these quantities is unknown. It was however demonstrated that it is difficult to make the inferred scaling of the perpendicular diffusivity match that from the global energy confinement time. The magnitude of the predicted threshold for instability as predicted by the $\chi_\perp/\chi_{||}$ model is much lower than that observed in the experiment. Therefore we conclude that the $\chi_\perp/\chi_{||}$ model alone is not capable of explaining the observed threshold for instability in COMPASS-D, but that the ion polarisation current model is consistent with present observations. The analysis is simple, based on estimates of the appropriate local quantities taken from fixed scalings to globally measured quantities (both β and density). These results require closer scrutiny, preferably with direct measurements of the required local parameters, but the general conclusions are unlikely to change.

The existence of a critical β_p which is a strong function of the plasma density has been verified experimentally, and is in both quantitative and qualitative agreement with the ion polarisation current stabilising term. These results can also be taken to be strong evidence of the importance of the bootstrap current and ion polarisation current in determining tearing mode stability. A corollary to the observation of the existence of a critical β_p is the observation of a reduction in the size of the error field for the mode to penetrate the plasma when $\beta_p > \beta_{pcrit}$, a phenomenon not yet well explained by the theory of error fields in plasmas.

A model has been developed based on the assumption of a maximum allowable island width determined by either the distance from the mode rational surface to the plasma edge or from the mode rational surface to an interior surface (e.g. the $q=1$ surface). The agreement between the prediction of this simple model and the observed β limit is remarkable, particularly in light of the simplicity of the model. Once again the analysis should be done in more detail using measurements of the relevant profile quantities.

It is important to note that neoclassical modes do not represent an absolute limit to β, since they are not "unstable" in the true sense of the word. They are instead metastable, requiring a perturbation to trigger instability. The β-limit can be raised by either operating in a regime where they are not excited, or by modifying profiles (see Reference [2]) to mitigate their effect. By avoiding neoclassical modes, $\beta_N > 2.1$ has been achieved in COMPASS-D discharges with 2nd Harmonic ECRH with line averaged densities $\sim 1.2 \times 10^{19} m^{-3}$.

These results, when combined with the detailed calculations in References [8] and [17] using measured experimental profiles, provide a strong confirmation that the operational limit to β can often be due to bootstrap current driven magnetic islands and that the ion polarisation current is a likely explanation for the collisionality scaling of the onset of neoclassical islands.

ACKNOWLEDGEMENTS

We would like to thank the COMPASS-D and ECRH teams team for operating the tokamak. This work was jointly funded by the UK Department of Trade and Industry and EURATOM.

12. References

[1] F. TROYON, J. GRUBER, H. SAURENMANN, S. SEMENZATO, S. SUCCI, Plas. Phys. and Cont. Fus. **26** (1984) 209

[2] GATES, D. A., et al., in Controlled Fusion and Plasma Physics (Proc. 22nd Eur. Conf. Bournemouth, 1995) **19C**, Part IV, EPS, Geneva, (1995) 117.

[3] LaHAYE, R., et al., submitted to Nucl. Fus. (1996)

[4] ZOHM, H., et al., Plas. Phys. Cont. Fus. **37** (1995) A313

[5] Y. KAMADA, et al., To be published in *Proceedings of the 16th International Fusion Energy Conference, Montreal,* 1996, IAEA-CN-64/A1-6

[6] See National Technical Information Service Document No. DE6008946 (W. Q. XU and J. D. CALLEN, University of Wisconsin Plasma Report No. UWPR 85-5, 1985)

[7] CARRERA, R., et al., Phys. Fluids **29** (1986) 899

[8] CHANG, Z. et al., Phys. Rev. Lett. **74** (1994) 4663

[9] FITZPATRICK, R., Phys. Plasmas **2** (1995) 825

[10] SMOLYAKOV, A. I., et al., Phys. Plasmas **2** (1995) 1581

[11] WILSON, H. R., et al., Phys. Plasmas **3** (1996) 248

[12] O'BRIEN, M. R., et al., IAEA Technical Committee Meeting on Advances in Modelling Plasmas, Montreal (1992), 527

[13] GORELENKOV, N. N., et al., Phys. Plasmas **3** (1996) 3379

[14] MORRIS, A. W. et al., Phys. Fluids B **4** (1992) 413

[15] GATES, D. A., et al., To be published in *Proceedings of the 16th International Fusion Energy Conference, Montreal,* 1996, IAEA-CN-64/AP1-17

[16] FISHPOOL, G. M., and Haynes, P. S., Nucl. Fus. **34**, (1994) 109

[17] WILSON, H.R., et al., Plas. Phys. Cont. Fus., **38** (1996) A149

Figure Captions

Figure 1. Figure showing the typical behaviour of Equations (1) and (3) for COMPASS-D parameters. Steady state solutions are represented by the zero crossings. The introduction of a "threshold" as in Equation (3), creates a stable region at small island width. The values of w_c (in the curve where $a_2 = 0$) and a_2 (in the curve where $w_c = 0$) were chosen so as to give the same threshold island width.

Figure 2 a) Figure showing the effect of an increase in β_p on the solutions to Equation (3) for the case where $w_c = 0$ (keeping $\rho_{\theta i}$ constant). b) same as a) but with $w_c > 0$ and $a_2 = 0$. c) the effect of varying the function $g(\varepsilon)$ for fixed β_p with $w_c = 0$. The values of the other relevant quantities were chosen to reflect typical COMPASS-D conditions.

Figure 3 Equilibrium reconstruction of a typical ITER-like COMPASS-D discharge shown inside the COMPASS-D vacuum vessel. Also shown is a high field side antenna and the ECRH rays for all the antennae as traced by the BANDIT3D Fokker-Planck code. The crosses indicate power absorption

Figure 4 Data from plasma with a large saturated neoclassical island for which the input power (and hence β_p) is ramped down: a) the measured Mirnov amplitude, b) the

input power and β_p (as measured by diamagnetic loop) and the fit to β_p used in the modelling, and c) the measured island width (solid trace) overlaid with the predicted island width (dashed trace) as calculated by a code that solves Equation (3). The coefficients used in the fit are: $r_s\Delta' = -2.0$, $a_1 = a_2 = 7.0$. The experimental parameters for the discharge are $B_\phi = 1.2$T, $m/n = 2$, $\varepsilon = 0.25$, $Z_{eff} \sim 2.0$, $m = 2$, $R_0 = 0.56$m, and $n_e = 1.0\text{x}10^{19}\text{m}^{-3}$.

Figure 5 Data from a typical discharge in the density scan: a) plasma current, b) ECRH power, c) β_p as measured by diamagnetic loop, d) measured loop voltage (which drops to >10mV indicating a strong bootstrap current).

Figure 6 Mirnov activity for four example discharges in the density scan. As the density is raised, the onset of MHD is delayed. The β_p and the density at the point of the onset of MHD are shown in each frame of the figure. β_p is ramped across each frame and the time history is very similar for all the discharges.

Figure 7 The early time behaviour of the growth of a 2/1 neoclassical island. The onset of the mode correlates with a sawtooth (the time of the sawtooth crash is indicated). The second frame shows the root mean square of 12 coils summed in such a way as to enhance the signal to noise for a 2/1 mode.

Figure 8 The time derivative of the island width as calculated from the data from Figure 7 vs. the island width. The smooth curve is the curve predicted by Equation (3). The numbered points in the figure correspond to the numbered points in Figure 7.

Figure 9 Measured threshold island width for the density scan plotted against a) density and b) β_p. This indicates that the size of the available perturbation due to sawteeth is not varying strongly as these quantities are varied.

Figure 10 The magnitude of the threshold island width as a function of β_p and density. The horizontal lines represent the critical β_p (which is a function of the collisionality parameter $\nu_i/\varepsilon\omega_{*e}$) below which the mode is always stable. The parabolic curve is the boundary between low and high "collisionality" as determined by the collisionality parameter $\nu_i/\varepsilon\omega_{*e} = 0.3$. The full circles represent the point of onset of MHD for the data from the density scan. Local quantities are calculated from the global quantities by assuming parabolic temperature and density profiles.

Figure 11 Data from a power scan in the "collisional" region with islands induced by an applied 2/1 quasi-helical error field, a-d) the time history of the measured n = odd perturbed radial magnetic field for a series of shots at fixed density with different β_p.

Figure 12 The density and β_p at the point of penetration of a resonant applied $m = 2$, $n = 1$ error field. Also shown are the data and threshold curves from Figure 10.

Figure 13 The maximum achieved β_N as a function of q_{95} for a series of discharges, all of which have large $m = 2$, $n = 1$ islands. The solid curve is that predicted by the relationship in Equation (23). Note that this limit is only applicable if neoclassical modes are present, higher β_p can be acheived by careful programming of the plasma.

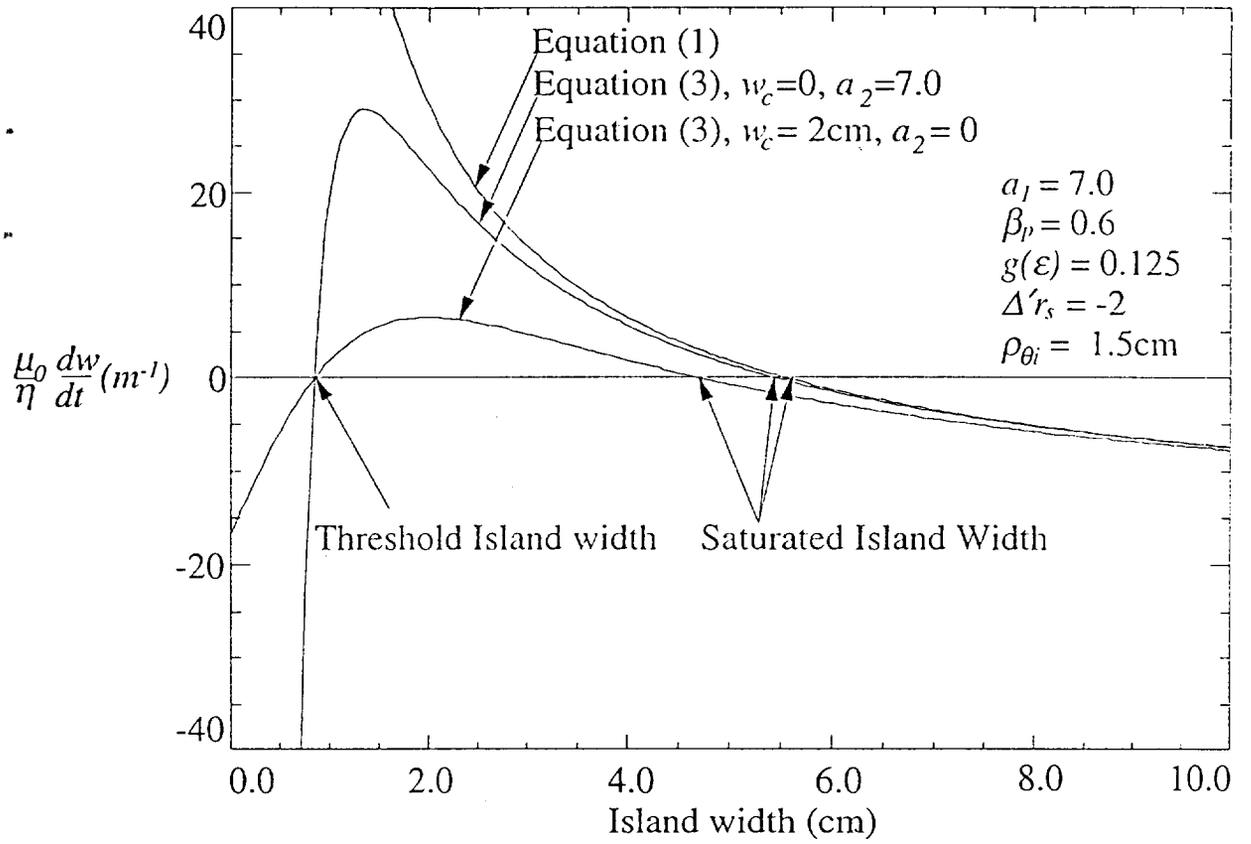
Equation (1)
Equation (3), w_c=0, a_2=7.0
Equation (3), w_c= 2cm, a_2= 0
a_1 = 7.0
β_p = 0.6
$g(\varepsilon)$ = 0.125
$\Delta' r_s$ = -2
$\rho_{\theta i}$ = 1.5cm
Threshold Island width
Saturated Island Width
$\frac{\mu_0}{\eta}\frac{dw}{dt}(m^{-1})$
40
20
0
-20
-40
0.0
2.0
4.0
6.0
8.0
10.0
Island width (cm)

Figure 1

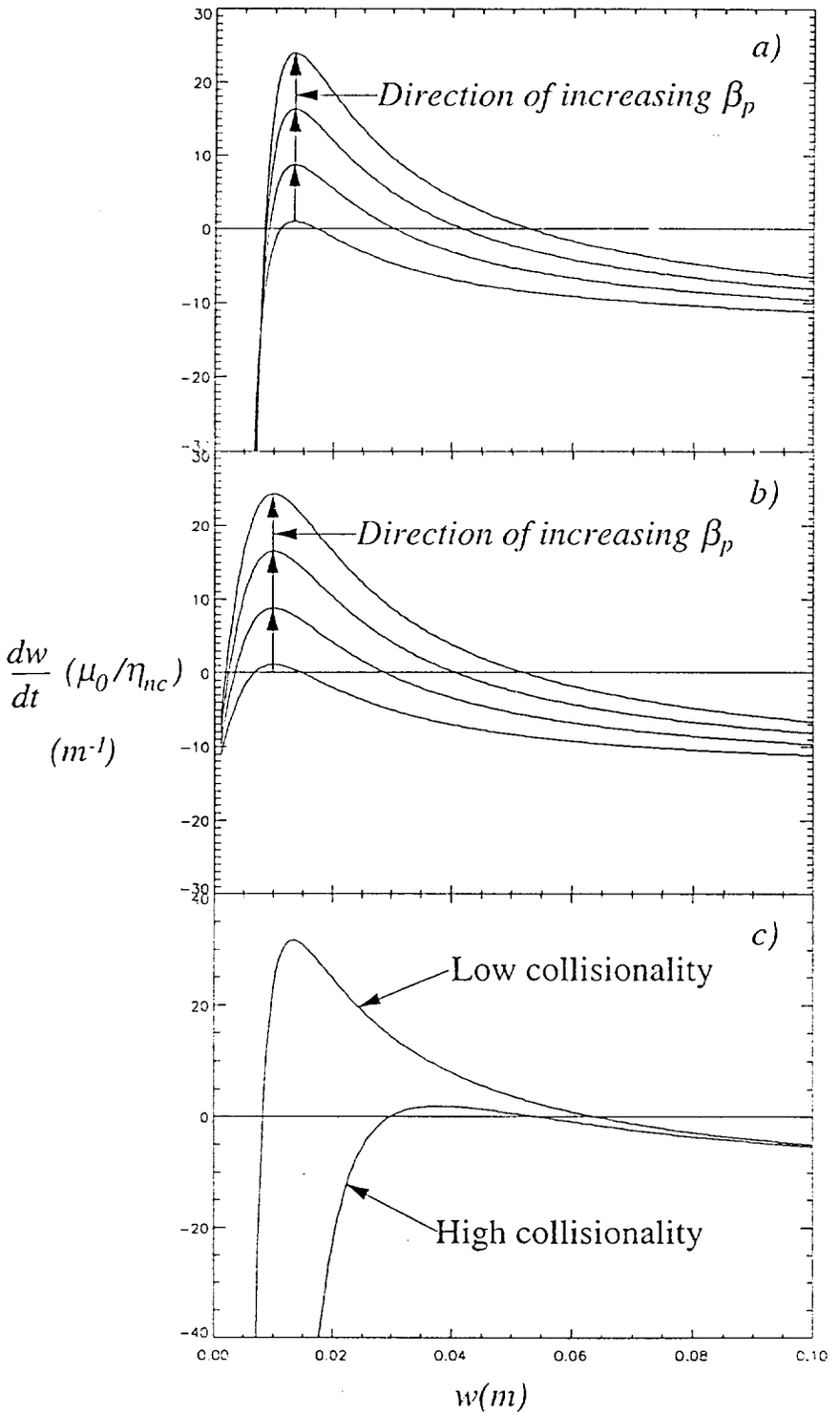
a)
Direction of increasing β_p
b)
Direction of increasing β_p
c)
Low collisionality
High collisionality
$\frac{dw}{dt}\ (\mu_0/\eta_{nc})$
(m^{-1})
$w(m)$
30
20
10
0
-10
-20
-30
-40
0.00
0.02
0.04
0.06
0.08
0.10

Figure 2

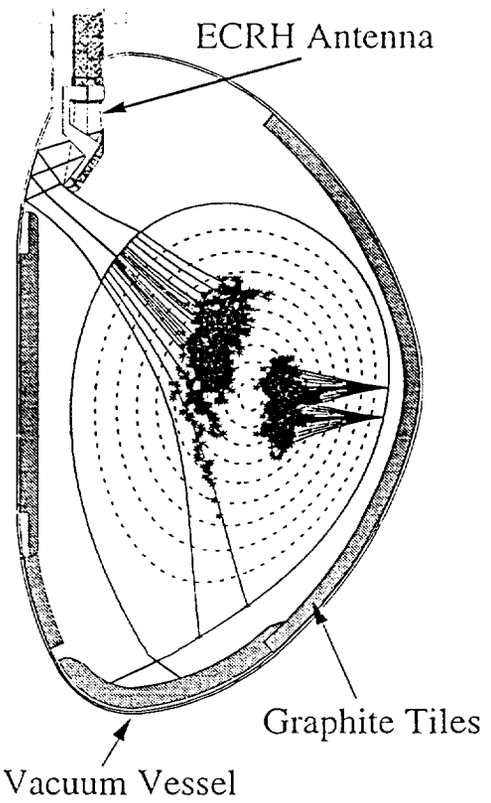

Figure 3

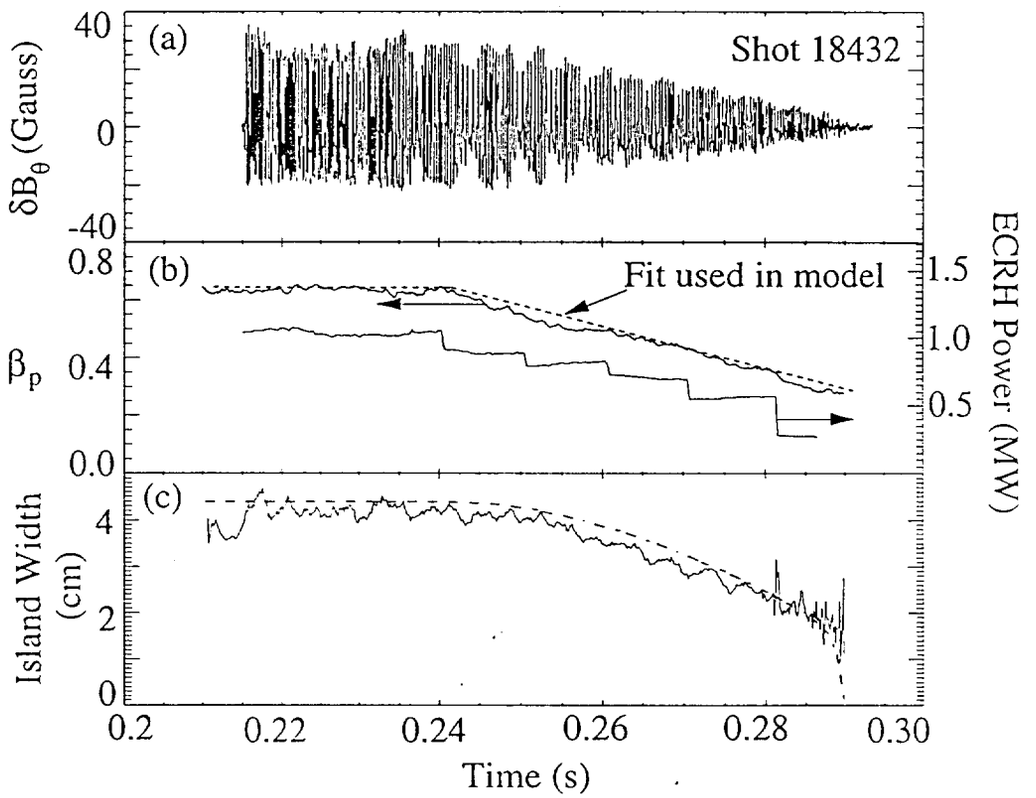
(a)
Shot 18432
40
0
-40
δB_θ (Gauss)
(b)
Fit used in model
0.8
0.4
0.0
β_p
1.5
1.0
0.5
ECRH Power (MW)
(c)
4
2
0
Island Width (cm)
0.2
0.22
0.24
0.26
0.28
0.30
Time (s)

Figure 4

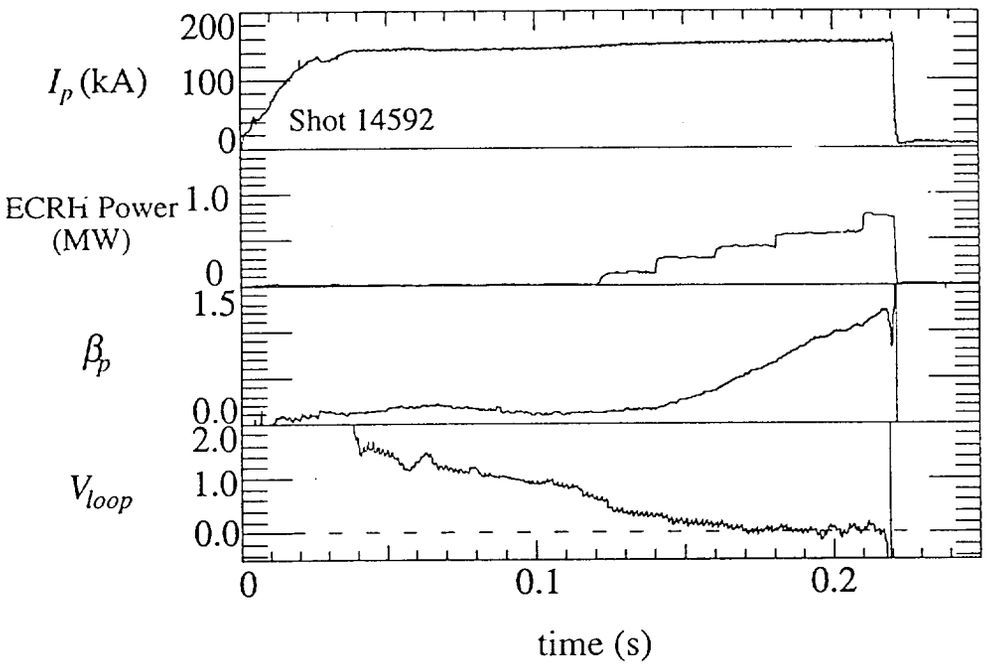
200
I_p (kA) 100
0
Shot 14592
ECRH Power 1.0
(MW)
0
1.5
β_p
0.0
2.0
V_{loop} 1.0
0.0
0
0.1
0.2
time (s)

Figure 5

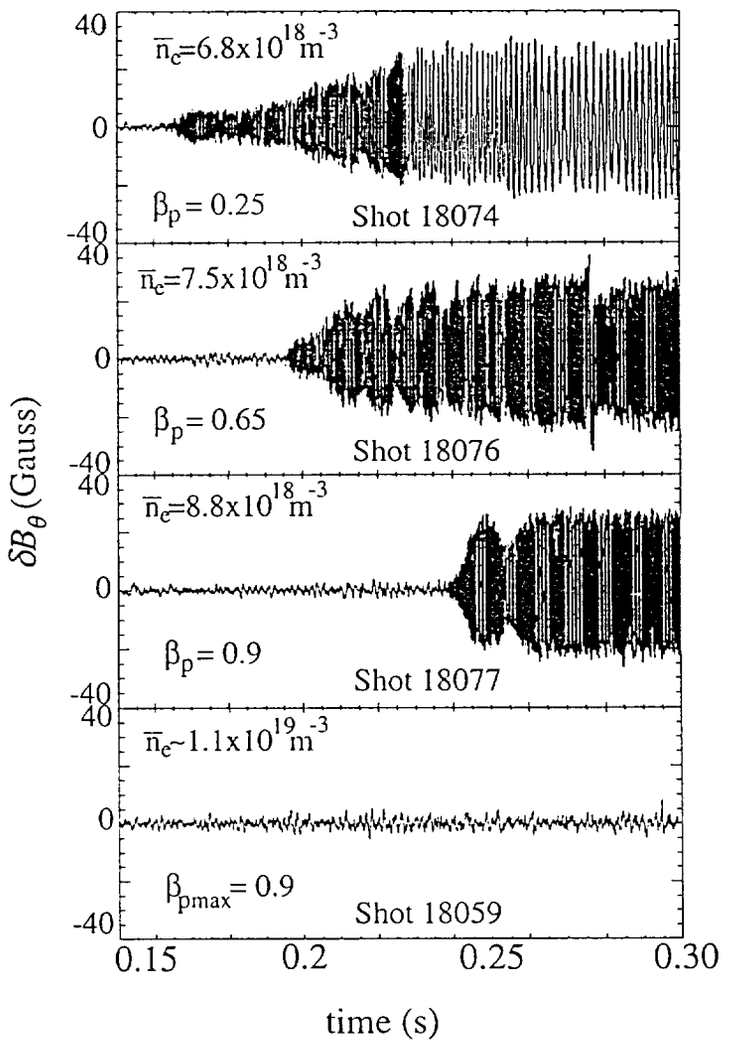
40
0
-40
$\bar{n}_e$=6.8x10^{18}m^{-3}
β_p = 0.25
Shot 18074
$\bar{n}_e$=7.5x10^{18}m^{-3}
β_p= 0.65
Shot 18076
$\bar{n}_e$=8.8x10^{18}m^{-3}
β_p= 0.9
Shot 18077
$\bar{n}_e$~1.1x10^{19}m^{-3}
β_{pmax}= 0.9
Shot 18059
δB_θ (Gauss)
0.15
0.2
0.25
0.30
time (s)

Figure 6

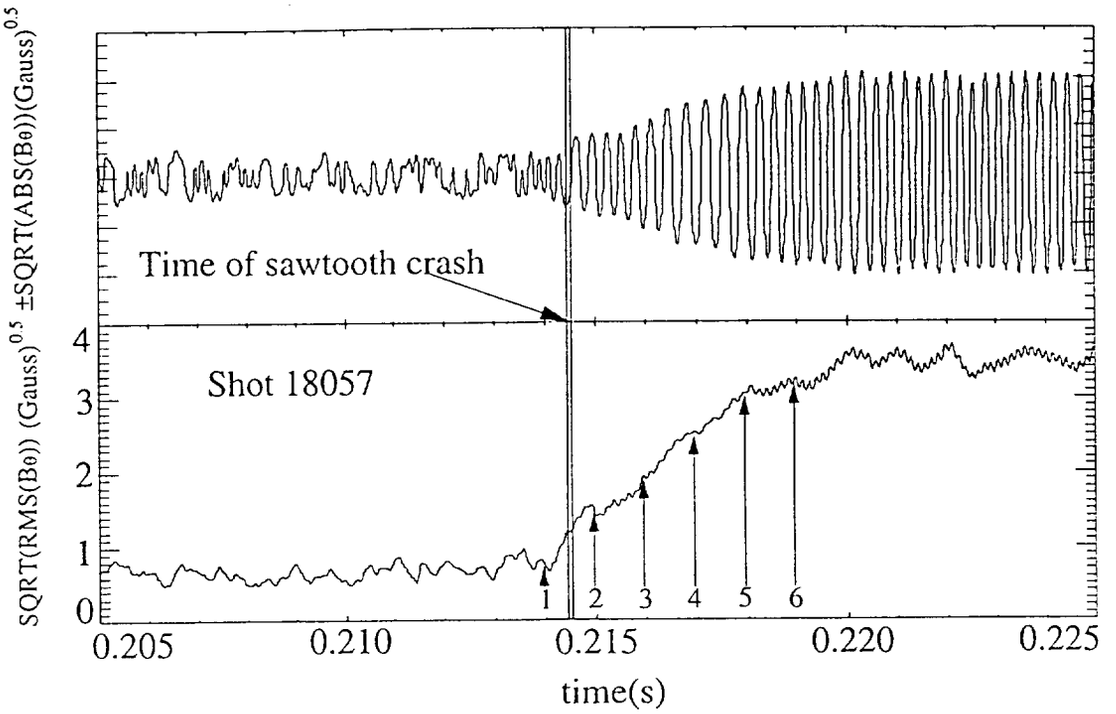

Figure 7

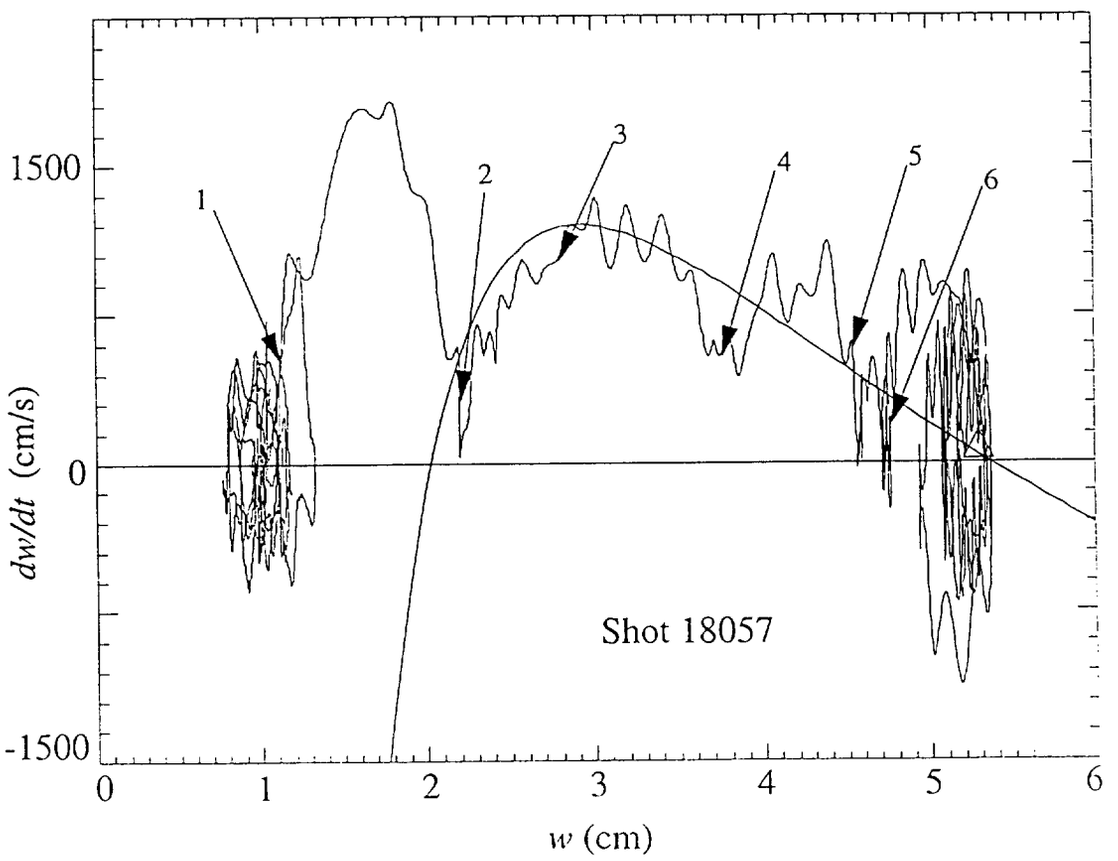

Figure 8

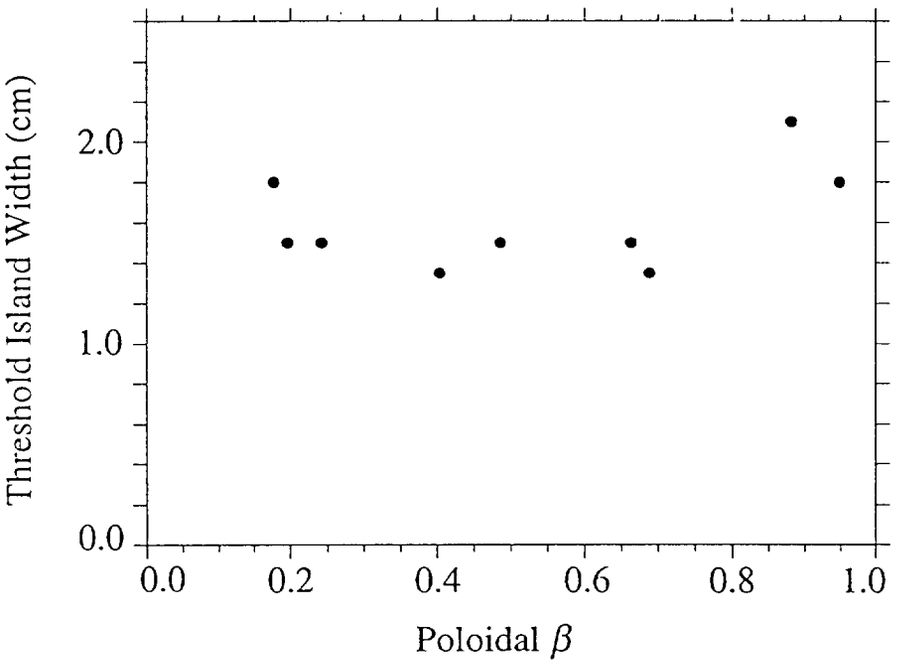
Threshold Island Width (cm)
2.0
1.0
0.0
0.0
0.2
0.4
0.6
0.8
1.0
Poloidal β

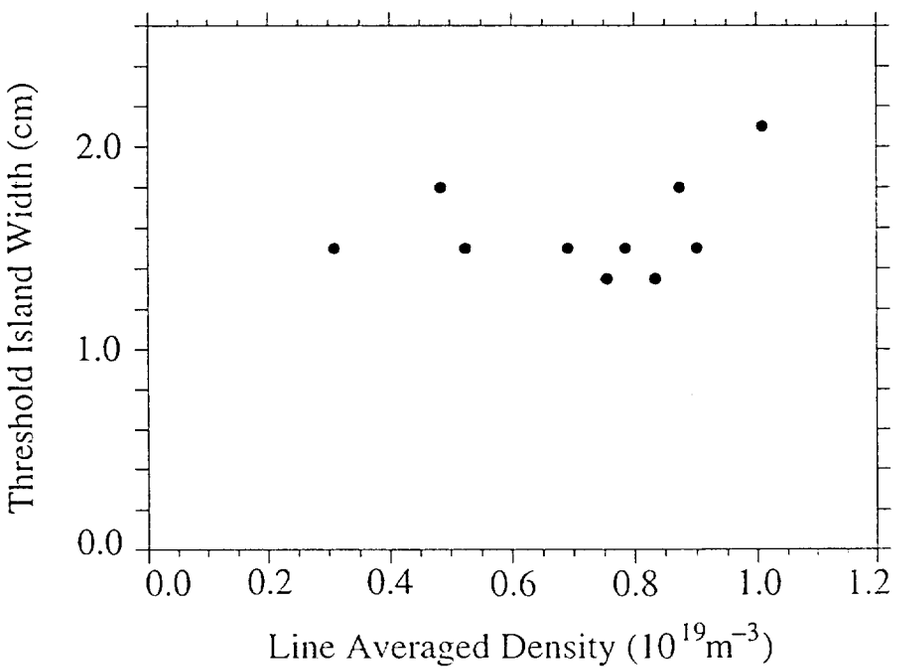
Threshold Island Width (cm)
2.0
1.0
0.0
0.0
0.2
0.4
0.6
0.8
1.0
1.2
Line Averaged Density ($10^{19}m^{-3}$)

Figure 9

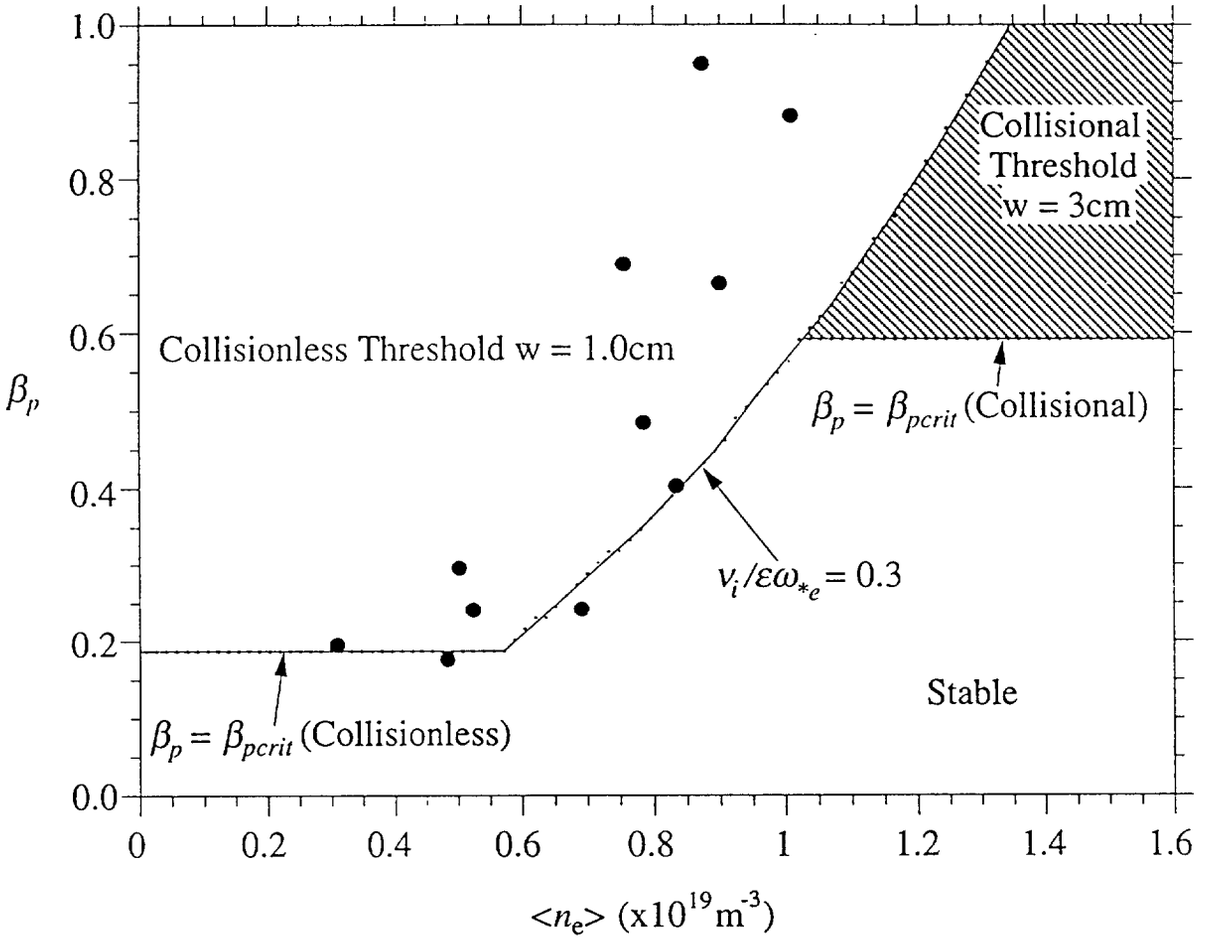
1.0
0.8
0.6
0.4
0.2
0.0
β_p
Collisional
Threshold
w = 3cm
Collisionless Threshold w = 1.0cm
$\beta_p = \beta_{pcrit}$ (Collisional)
$\nu_i/\varepsilon\omega_{*e} = 0.3$
Stable
$\beta_p = \beta_{pcrit}$ (Collisionless)
0
0.2
0.4
0.6
0.8
1
1.2
1.4
1.6
$\langle n_e \rangle$ (x10^{19}m^{-3})

Figure 10

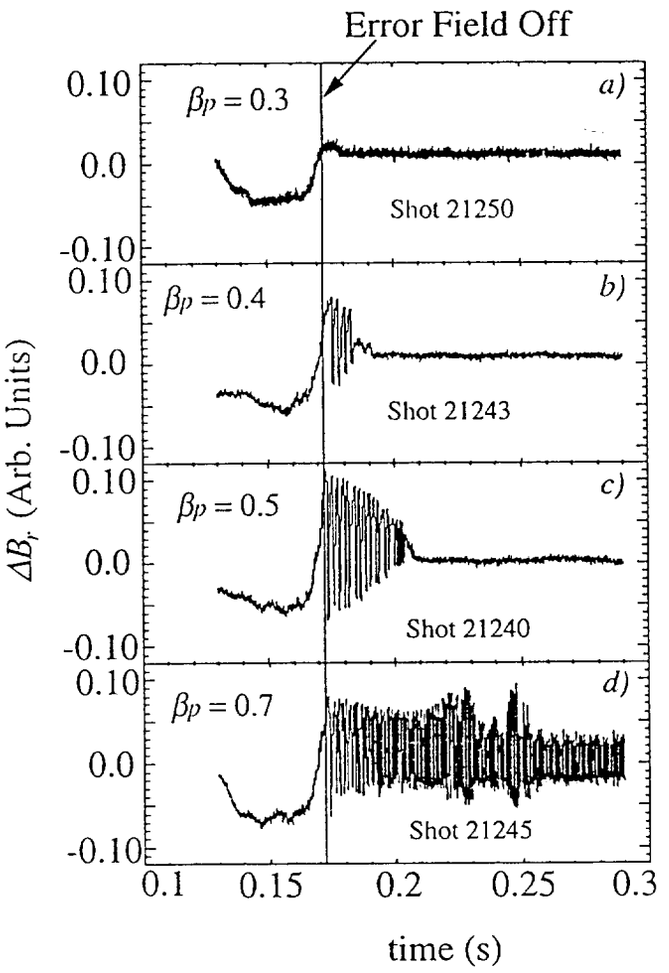
Error Field Off
0.10
0.0
-0.10
$\beta_p = 0.3$
a)
Shot 21250
$\beta_p = 0.4$
b)
Shot 21243
$\beta_p = 0.5$
c)
Shot 21240
$\beta_p = 0.7$
d)
Shot 21245
ΔB_r (Arb. Units)
0.1
0.15
0.2
0.25
0.3
time (s)

Figure 11

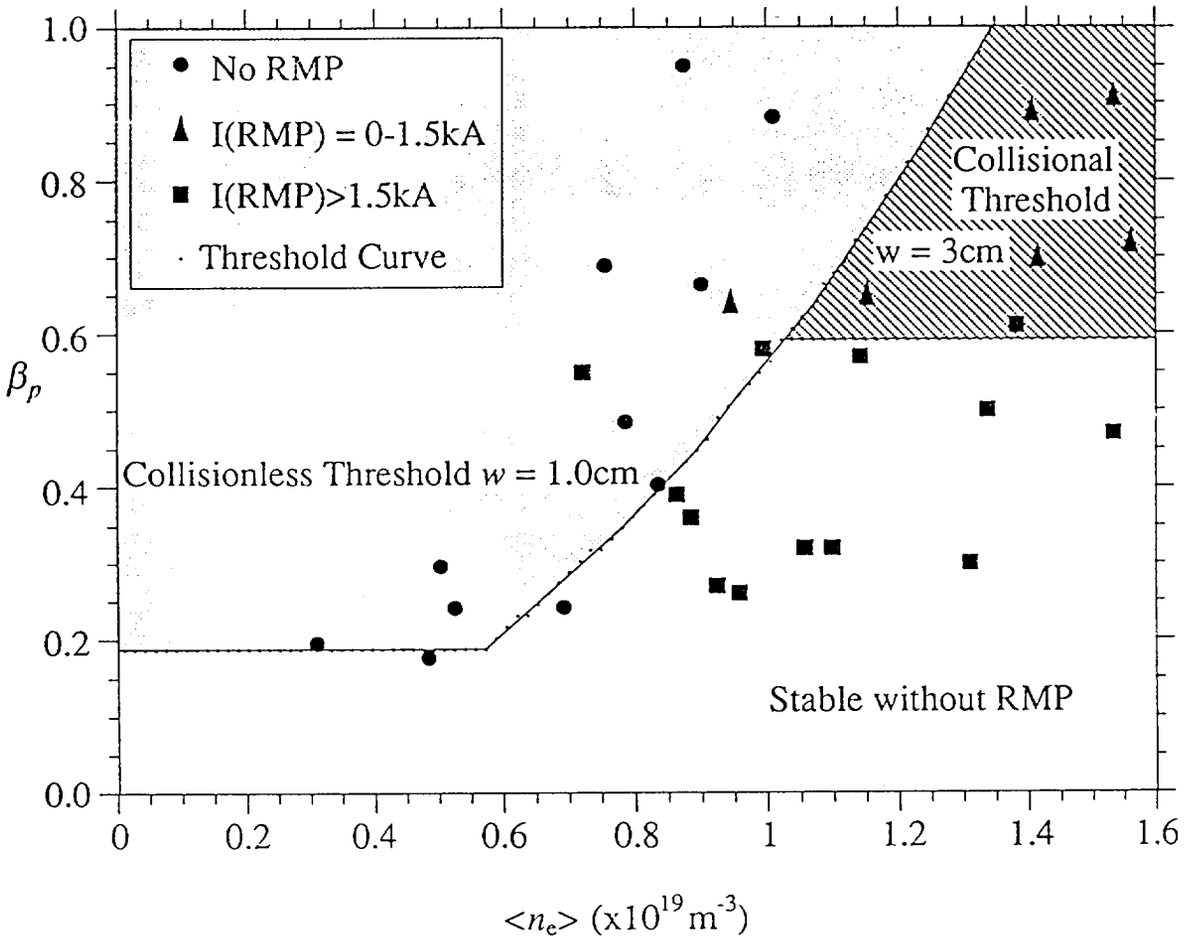
No RMP
I(RMP) = 0-1.5kA
I(RMP)>1.5kA
Threshold Curve
Collisional
Threshold
w = 3cm
Collisionless Threshold w = 1.0cm
Stable without RMP
β_p
$<n_e>$ (x10^{19} m^{-3})
1.0
0.8
0.6
0.4
0.2
0.0
0
0.2
0.4
0.6
0.8
1
1.2
1.4
1.6

Figure 12

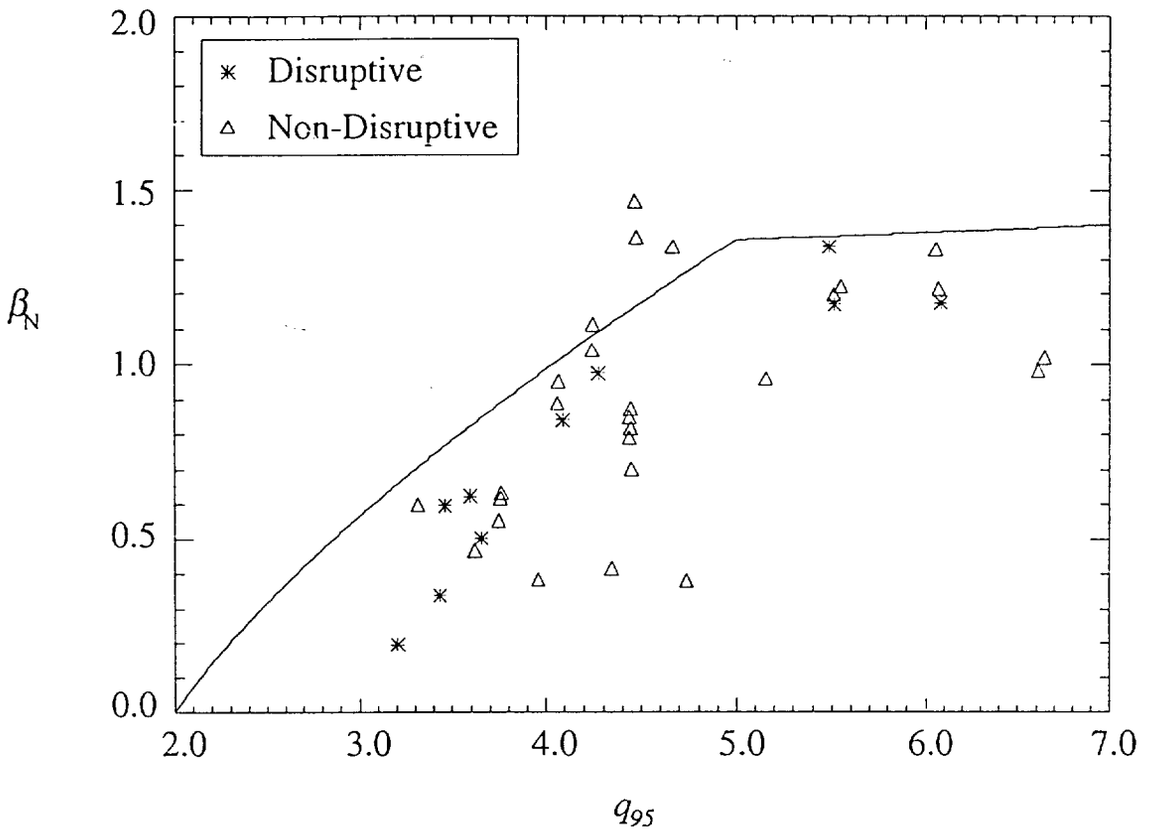
Disruptive
Non-Disruptive
2.0
1.5
1.0
0.5
0.0
β_N
2.0
3.0
4.0
5.0
6.0
7.0
q_{95}

Figure 13